

Alzheimer's disease genetic pathways impact cerebrospinal fluid biomarkers and imaging endophenotypes in non-demented individuals

Lorenzini, Luigi; Collij, Lyduine E.; Tesi, Niccoló; Vilor-Tejedor, Natàlia; Ingala, Silvia; Blennow, Kaj; Foley, Christopher; Frisoni, Giovanni B.; Reinders, Marcel; More Authors

DOI

[10.1002/alz.14096](https://doi.org/10.1002/alz.14096)

Publication date

2024

Document Version

Final published version

Published in

Alzheimer's and Dementia

Citation (APA)

Lorenzini, L., Collij, L. E., Tesi, N., Vilor-Tejedor, N., Ingala, S., Blennow, K., Foley, C., Frisoni, G. B., Reinders, M., & More Authors (2024). Alzheimer's disease genetic pathways impact cerebrospinal fluid biomarkers and imaging endophenotypes in non-demented individuals. *Alzheimer's and Dementia*, 20(9), 6146-6160. <https://doi.org/10.1002/alz.14096>

Important note

To cite this publication, please use the final published version (if applicable).
Please check the document version above.

Copyright

Other than for strictly personal use, it is not permitted to download, forward or distribute the text or part of it, without the consent of the author(s) and/or copyright holder(s), unless the work is under an open content license such as Creative Commons.

Takedown policy

Please contact us and provide details if you believe this document breaches copyrights.
We will remove access to the work immediately and investigate your claim.

RESEARCH ARTICLE

Alzheimer's disease genetic pathways impact cerebrospinal fluid biomarkers and imaging endophenotypes in non-demented individuals

Luigi Lorenzini^{1,2}  | Lyduine E. Collij^{1,2,3} | Niccoló Tesi^{2,4,5} |
 Natàlia Vilor-Tejedor^{6,7,8,9} | Silvia Ingala^{10,11} | Kaj Blennow^{12,13} | Christopher Foley¹⁴ |
 Giovanni B. Frisoni^{15,16} | Sven Haller^{17,18,19} | Henne Holstege⁴ | Sven van der
 van der Lee^{4,20} | Pablo Martinez-Lage²¹ | Riccardo E. Marioni²² |
 Daniel L. McCartney²² | John O'Brien²³ | Tiago Gil Oliveira^{24,25} | Pierre Payoux^{26,27} |
 Marcel Reinders⁵ | Craig Ritchie^{28,29} | Philip Scheltens²⁰ | Adam J. Schwarz³⁰ |
 Carole H. Sudre^{31,32,33} | Adam D. Waldman^{34,35} | Robin Wolz³⁶ | Gael Chatelat³⁷ |
 Michael Ewers³⁸ | Alle Meije Wink^{1,2} | Henk J. M. M. Mutsaerts^{2,39} |
 Juan Domingo Gispert^{6,7,40,41} | Pieter Jelle Visser^{20,42,43,44} | Betty M. Tijms^{20,42} |
 Andre Altmann⁴⁵ | Frederik Barkhof^{1,46}

Correspondence

Luigi Lorenzini, Department of Radiology and
 Nuclear Medicine, De Boelelaan 1117, 1081
 HV Amsterdam, the Netherlands.
 Email: l.lorenzini@amsterdamumc.nl

Funding information

EU/EFPIA Innovative Medicines Initiative
 Joint Undertaking EPAD, Grant/Award
 Number: 115736

Abstract

INTRODUCTION: Unraveling how Alzheimer's disease (AD) genetic risk is related to neuropathological heterogeneity, and whether this occurs through specific biological pathways, is a key step toward precision medicine.

METHODS: We computed pathway-specific genetic risk scores (GRSs) in non-demented individuals and investigated how AD risk variants predict cerebrospinal fluid (CSF) and imaging biomarkers reflecting AD pathology, cardiovascular, white matter integrity, and brain connectivity.

RESULTS: CSF amyloidbeta and phosphorylated tau were related to most GRSs. Inflammatory pathways were associated with cerebrovascular disease, whereas quantitative measures of white matter lesion and microstructure integrity were predicted by clearance and migration pathways. Functional connectivity alterations were related to genetic variants involved in signal transduction and synaptic communication.

DISCUSSION: This study reveals distinct genetic risk profiles in association with specific pathophysiological aspects in predementia stages of AD, unraveling the biological substrates of the heterogeneity of AD-associated endophenotypes and promoting a step forward in disease understanding and development of personalized therapies.

This is an open access article under the terms of the [Creative Commons Attribution-NonCommercial-NoDerivs](https://creativecommons.org/licenses/by-nc-nd/4.0/) License, which permits use and distribution in any medium, provided the original work is properly cited, the use is non-commercial and no modifications or adaptations are made.

© 2024 The Author(s). *Alzheimer's & Dementia* published by Wiley Periodicals LLC on behalf of Alzheimer's Association.

KEYWORDS

biological pathways, magnetic resonance imaging, polygenic risk, preclinical Alzheimer's disease

Highlights

- Polygenic risk for Alzheimer's disease encompasses six biological pathways that can be quantified with pathway-specific genetic risk scores, and differentially relate to cerebrospinal fluid and imaging biomarkers.
- Inflammatory pathways are mostly related to cerebrovascular burden.
- White matter health is associated with pathways of clearance and membrane integrity, whereas functional connectivity measures are related to signal transduction and synaptic communication pathways.

1 | BACKGROUND

Recent genome-wide association studies (GWASs) of sporadic Alzheimer's disease (AD) and related dementias¹ have identified more than 70 genetic variants that modify the risk of developing AD, beyond apolipoprotein E (APOE) $\epsilon 2/\epsilon 4$. These risk variants are involved in several pathophysiological pathways, such as amyloid-beta 1-42 ($A\beta_{1-42}$) production and clearance, lipid metabolism, endocytosis, immune function, and inflammatory response.² The multitude of pathophysiological processes involved in AD pathogenesis may explain heterogeneity in neuropathological features of AD that are already present in the pre-dementia stage.^{3,4} For example, individuals along the AD clinical spectrum can present with heterogeneous profiles of brain functional, structural, and cerebrovascular alterations observed through magnetic resonance imaging (MRI) techniques.^{5,6} Neuropathological heterogeneity further exacerbates disease complexity and may contribute to the partial efficacy of anti-amyloid compounds investigated in clinical trials for AD.⁷ Individuals in the early stages of the AD continuum might indeed present alterations in different biological pathways, eventually leading to heterogeneous neuroimaging and clinical manifestations.⁸ Characterizing how genotype influences heterogeneity in these imaging phenotypes is essential for understanding individual differences in disease cause, presentation, trajectory, and response to treatment,⁹ thus will be necessary for patients' selection and stratification in clinical trials.

One way to link genetic variants to biological pathways and neuropathological features is through determining total and pathway-specific genetic risk scores (GRSs). GRSs are weighted scores that quantify the individual genetic predisposition to develop a disease, such as AD, calculated by computing the sum of risk alleles that an individual has, weighted by the risk allele effect sizes as estimated by a GWAS.¹⁰ Furthermore, by linking variants to genes, and genes to associated biological pathways, one can compute pathway-specific GRSs (pathway-GRSs), which retain information about how the burden of genetic risk varies across biological processes.¹¹

The APOE- $\epsilon 4$ genotype promotes amyloid deposition during the stages preceding dementia onset,¹² and has been associated, although less consistently, with tau deposition,¹³ hippocampal atrophy,¹⁴ and alterations of functional connectivity (FC).¹⁵ In contrast, there is scant evidence linking early fluid and imaging AD-related traits to genetic pathways beyond APOE. It has been demonstrated that the cerebrospinal fluid (CSF) phosphorylated tau (p-tau) and total tau (t-tau) levels are correlated with GRSs for AD that did not include the APOE variants.¹⁶ Moreover, GRSs have been associated with higher rates of tau-PET (positron emission tomography) and amyloid-PET uptake in patients with AD, independently of APOE genotype.¹⁷ Pathway-GRSs of endocytosis and immune response have been found to be associated with AD clinical progression, and to a lower extent with imaging markers of white matter damage.¹⁸ Although this suggests that certain AD phenotypes may be preferentially associated with accumulated genetic risk along particular biological pathways, current research has mostly focused on specific aspects, failing to capture genetic bases and pathways that regulate the broad spectrum of imaging and molecular biomarkers changes in preclinical AD stages.

To assess the genetic vulnerability underlying early AD-associated changes in brain pathology, structure, and function, we tested whether GRSs and pathways-GRSs of Alzheimer's disease and related dementias¹ relate to (1) CSF levels of $A\beta_{1-42}$ and p-tau₁₈₁, (2) radiological features of cerebral small-vessel disease (cSVD), and (3) a broad set of quantitative imaging phenotypes from multimodal MRI.

2 | METHODS

2.1 | Participants

Data were drawn from the latest data release from the European Prevention of Alzheimer's Dementia (EPAD) multicenter study.¹⁹ EPAD general inclusion criteria were age older than (or equal to) 50 years and no diagnosis of dementia (Clinical Dementia Rating [CDR] scale

RESEARCH IN CONTEXT

1. **Systematic review:** Polygenic risk for Alzheimer's disease (AD) comprises genetic variants that play a role in various biological processes, extending beyond amyloid production and clearance. This broader genetic influence may account for the heterogeneity of neuropathological observed from the early stages of the disease. Understanding these distinct pathophysiological pathways is crucial for comprehending the disease and tailoring treatments to individual patients.
2. **Interpretation:** Using data from a large multicenter cohort study, we demonstrate that distinct genetic profiles determine specific imaging abnormalities and promote disease heterogeneity, through differential biological pathways.
3. **Future directions:** Pathway-specific genetic profiling may offer novel perspectives for patient stratification and precision medicine.

score <1). Exclusion criteria were the presence of conditions associated with neurodegeneration or affecting cognition, contraindication to MRI or lumbar puncture, and cancer or history of cancer in the preceding 5 years. A total of 1835 participants were included in the EPAD study. Demographic, cognitive, neuroimaging, fluid biomarker, and genetic outcome data were collected.²⁰ For this work, we excluded participants with unavailable or low-quality (see below) genetic data, resulting in a final sample of $n = 1738$.

2.2 | Genetic data acquisition and processing

DNA samples were genotyped using Illumina Infinium Global Screening Array-24 v3.0. Standard quality control procedures were applied using PLINK (www.cog-genomics.org) and are available online (<https://github.com/marioni-group/epad-gwas>). Briefly, quality control ensured high-quality genotypes in all individuals (individual call rate >99%, variant call rate >99%), excluding single nucleotide polymorphisms (SNPs) with a significant departure from Hardy–Weinberg equilibrium ($p < 1 \times 10^{-10}$) and keeping SNPs with minor allele frequency >0.5%. Before imputation, individuals of non-European ancestry ($n = 19$, based on clustering with HapMap III reference data) and individuals with a family relation ($n = 46$, identity-by-descent >0.1875) were excluded. Genotypes were imputed using the Michigan Imputation Server (<https://imputationserver.sph.umich.edu>)²¹ against European sample data from the Haplotype Reference Consortium (HRC, v1.1, GRCh37). Analyses were restricted to SNPs with imputation quality scores (RSq) ≥ 0.6 and minor allele frequencies (MAFs) ≥ 0.0005 .

2.3 | Genetic risk scores calculation

We constructed GRSs using 85 variants that were previously significantly associated (genome-wide threshold) with AD and related dementias,¹ in a sample of individuals that had no overlap with the EPAD cohort. The variant effect sizes (log of odds ratio) reported in the original work (Table S1) were used as weights for the GRS. Given a subject s , the GRS is defined as:

$$PRS = \sum_{k=1}^K dosage_{ks} \times \ln(OR_k)$$

where K represents the full set of genetic variants, $dosage_{ks}^k$ denotes the allele dosage from the (imputed) genotype of variant k in subject s , and $\ln(OR_k)$ is the logarithmically transformed odds ratio of variant k .

To investigate the effects of genetic variants beyond APOE, GRSs were computed both with and without the two alleles (rs7412 and rs429358) from the APOE gene (denoted as GRS_{APOE} and GRS_{noAPOE} , respectively).

2.4 | Pathway-GRS

In order to construct pathway-specific GRSs, SNPs were mapped to pathways. We used a previously developed data-driven method,²² which has no a priori pathway definition and consists of two fundamental steps: first, single SNPs were linked to likely affected genes (variant-gene mapping); then, identified genes were associated with biological pathways (gene-pathway mapping). This method has previously demonstrated its capability to identify canonical disease pathways as identified in prior studies.²² The pathway analysis was performed on the set of SNPs excluding the APOE region, to specifically evaluate APOE-independent pathways.

2.4.1 | Variant-gene mapping

To perform the first step of this procedure we relied on the variant-gene mapping reported in the reference GWAS study.¹ Briefly, to prioritize candidate genes in the new loci, the authors integrated variant annotation, quantitative-trait-loci (QTL) (such as expression-QTL, protein-QTL, splicing-QTL, methylation-QTL, and histone acetylation-QTL), and β -amyloid precursor protein (APP) metabolism. Detailed information about the annotation procedure is reported in the original work. Prioritized genes are reported in Table S1.

2.4.2 | Gene-pathway mapping

A gene-set enrichment analysis was then performed with snpXplorer²² to find biological pathways enriched within the set of identified genes. The Gost function from the R package gprofiler2²³ was used with gene ontology²⁴ as a reference gene source for functional profiling.

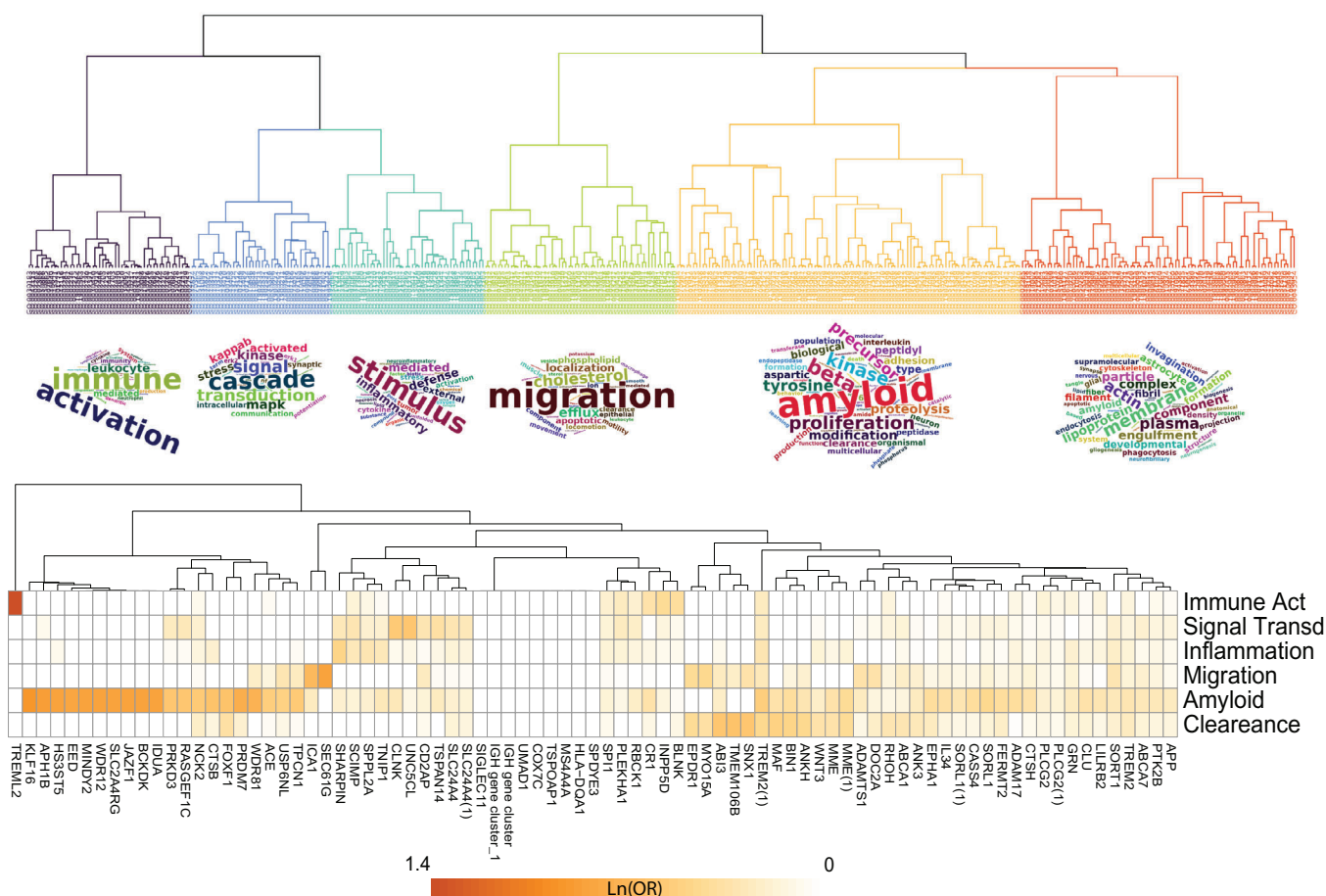


FIGURE 1 Results of the pathway analysis. The upper part of the figure shows the results of the clustering performed on identified pathways relating to the selected set of genes. The most frequent words from the pathways description within each cluster of pathways are visualized using word clouds. The lower part of the figure shows the contribution of each gene to each identified cluster, expressed as a log of odds ratios.

Briefly, snpXplorer calculates a semantic similarity matrix between all enriched pathways, which is then used in a hierarchical clustering framework to obtain clusters of similar pathways. Lin distance²⁵ is used as a semantic similarity metric, whereas the number of clusters is estimated with a dynamic cut-tree algorithm. By counting the number of times each SNP was associated with each cluster of pathways, and dividing by the total number of associations per SNP, we obtained a weighted mapping factor of each SNP to each cluster of pathways, varying between 0 and 1 and reflecting the contribution of that SNP to that cluster of pathways (Figure 1). In case no mapping to any of the pathways was found, we excluded the gene from further analyses.

2.4.3 | Pathway-GRSs

For the pathway-GRSs, we extended the definition of the GRS by adding as a multiplicative factor the variant-pathway-mapping weight of each variant:

$$GRS = \sum_{k=1}^K dosage_s^k \times \ln(OR_k) \times M_k^p$$

where M_k^p is the variant-pathway mapping of variant k to pathway p ,

thus obtaining N pathway GRSs estimates per subject, with N being the number of identified clusters.

2.5 | CSF analysis and AT classification

CSF biomarkers were quantified using a harmonized pre-analytical protocol. Analyses were performed with the fully automatized Roche cobas Elecsys System at the Clinical Neurochemistry Laboratory, Mölndal, Sweden.²⁰ Concentrations of A β ₁₋₄₂ were determined using the manufacturer's guidelines. Following a previous study on the same cohort,²⁶ CSF A β ₁₋₄₂ levels <1000 pg/mL were used to define amyloid positivity (A+), and CSF p-tau levels >27 pg/mL were used to define tau positivity (T+). Four AT groups were derived to define A–T–, A+T–, A+T+, and A–T+ participants.

2.6 | MRI acquisition and processing

EPAD MRI acquisition and pre-processing details are given in²⁷ and in supplementary materials. Briefly, at all sites the MRI protocol included acquisition of three-dimensional (3D) T1-weighted (3D T1w)

and 3D fluid-attenuated inversion recovery (FLAIR), 2D T2w, and 2D T2 star images. In a subset of sites, advanced MRI sequences were also acquired including resting-state functional MRI (rs-fMRI) and diffusion-weighted imaging (DWI). From T1w sequences, the learning embeddings for atlas propagation (LEAP)²⁸ framework was used to compute gray matter (GM) volumes in the hippocampus, normalized by the total intracranial volume (TIV). White matter hyperintensities (WMHs) were computed using Bayesian model selection (BaMoS)²⁹ on FLAIR sequences. Periventricular and deep WMH volumes were obtained globally and for the frontal, parietal, temporal, and occipital lobes,³⁰ and corrected for TIV to account for interindividual differences in total brain size. For rs-fMRI sequences, a dual regression approach³¹ was used to compute resting-state network FC within three subsystems of the default mode network (DMN),³² including a medial, dorsal, and ventral component, according to a previous study.³³ For DWI sequences, a tract-based spatial statistics (TBSS) approach was used to obtain regional values of fractional anisotropy (FA) and mean diffusivity (MD) in 10 WM tracts that have been shown previously to relate to Alzheimer's pathology. Examined WM tracts included commissural (genu, body, and splenium of corpus callosum), limbic (cingulum and fornix), associative (superior and inferior longitudinal fasciculus and superior fronto-occipital fasciculus), and projection (corona radiata and internal capsule) fibers.

2.7 | Radiological assessment

MRI radiological reads were centrally performed for all EPAD participants, following the STAndards for Reporting Vascular changes on nEuroimaging (STRIVE) criteria³⁴ to evaluate cSVD burden. Enlarged perivascular spaces (PVSs) in the basal ganglia (PVS-BG) and centrum semiovale (PVS-CS) were rated separately using a 0–4 interval scale on the 2D T2w images.³⁵ Visual rating of deep and periventricular WMH (DWMH and PVH, respectively) was performed using the 0–3 Fazekas scale on the FLAIR images.³⁶ Cortical microbleeds (CMBs) were classified as ≥ 2 or < 2 . A more detailed description of the used scales can be found in the supplementary materials.

2.8 | Statistical analyses

Data distributions were normalized before statistical analysis to meet linear model assumptions. Normalization steps are described in the supplementary materials. All the statistical models described below were corrected for age, sex, and population substructure (using the first five principal components computed on the genomic data). Models with the GRS_{noAPOE} and the pathway-GRSs as predictors were further corrected for APOE $\epsilon 4$ allele carriership to study independent effects. Participants in the A–T+ group were only included in the analysis of GRS differences across AT stages and otherwise excluded as considered suspected non-Alzheimer's pathology (SNAP).

2.8.1 | Association of GRSs with core AD features

First, we looked at the relationship between GRS and CSF biomarkers of AD. We used separate linear models to evaluate the association of global and pathway-GRSs with CSF $A\beta_{1-42}$ and p-tau₁₈₁ levels. Multinomial regression was used to study the association of global and pathway-GRSs with AT groups. In addition to the aforementioned corrections, models predicting CSF p-tau₁₈₁ were further corrected for $A\beta_{1-42}$. *p*-Values were corrected for multiple comparisons (Benjamini–Hochberg false discovery rate [FDR]).

2.8.2 | Association of GRSs with radiological imaging markers

The association of global and pathway-GRSs with radiological imaging markers, including radiological evaluation of the Fazekas score (PVH and DWMH; $n = 1595$), enlarged PVSs (BG and CS; $n = 1595$), and microbleeds ($n = 1595$) was investigated using multinomial and logistic (for microbleeds) regression models. The models were further adjusted for AT status.

2.8.3 | Association of GRSs with quantitative imaging markers

Quantitative imaging markers included hippocampal GM volumes (TIV normalized; $n = 1568$), global and lobar WMH volumes (10 regions; $n = 1334$), WM integrity (FA and MD) measures in the 10 selected tracts ($n = 790$), and FC within the three DMN subsystems ($n = 776$). Separate linear regression models were used to study the effect of global and pathway-GRSs on these variables. Besides the aforementioned corrections, models were adjusted for AT status and MRI scanner type. *p*-Values were corrected for multiple comparisons (Benjamini–Hochberg false discovery rate).

2.8.4 | Sensitivity analyses

Sensitivity analyses were performed to investigate the association between pathway-GRSs, the relationship of global and pathway-GRSs with age and sex, and the association of genetic scores with CSF biomarkers stratified by AT status.

3 | RESULTS

3.1 | Participants

Baseline demographics and clinical characteristics are shown in Table 1. In total, 1738 participants were included in the study. Based on CSF $A\beta_{1-42}$ and p-tau₁₈₁ levels, 58.5% ($n = 1016$) were defined as A–T–, 25.1% ($n = 436$) as A+T–, 9.2% ($n = 160$) as A+T+, and 7.2% ($n = 126$) as A–T+.²⁶ The 126 participants with SNAP, that is, A–T+, were used

TABLE 1 Cohort characteristics.

	Overall 1738	A–T– 1016	A–T+ 126	A+T– 436	A+T+ 160
Age, years , mean \pm SD	65.72 \pm 7.31	64.58 \pm 7.05	69.54 \pm 6.56	65.75 \pm 7.41	70.31 \pm 6.45
Sex, male, N (%)	767 (44.1)	425 (41.8)	55 (43.7)	208 (47.7)	79 (49.4)
MMSE, mean \pm SD	28.41 \pm 1.87	28.74 \pm 1.47	28.27 \pm 1.71	28.38 \pm 1.85	26.54 \pm 2.94
CDR = 0.5, N (%)	474 (27.4)	185 (18.3)	49 (38.9)	131 (30.0)	109 (68.1)
Education, years, mean \pm SD	14.37 \pm 3.71	14.49 \pm 3.57	13.95 \pm 3.81	14.55 \pm 3.80	13.44 \pm 4.09
GRS _{APOE} , mean \pm SD	0.22 \pm 0.72	0.04 \pm 0.63	0.30 \pm 0.74	0.38 \pm 0.75	0.79 \pm 0.75
GRS _{noAPOE} , mean \pm SD	–0.14 \pm 0.36	–0.16 \pm 0.35	–0.06 \pm 0.37	–0.14 \pm 0.37	–0.03 \pm 0.36
A β _{1–42} , mean \pm SD	1378.99 \pm 729.30	1672.06 \pm 496.43	2181.13 \pm 1320.89	724.48 \pm 186.27	669.82 \pm 177.00
p-tau ₁₈₁ , mean \pm SD	19.76 \pm 10.61	16.44 \pm 4.02	35.09 \pm 10.10	15.49 \pm 5.72	40.44 \pm 14.82
t-tau, mean \pm SD	226.85 \pm 99.33	198.27 \pm 45.87	392.01 \pm 101.13	181.01 \pm 58.60	399.96 \pm 117.78

Abbreviations: A β , amyloid beta; CDR, Clinical Dementia Rating (scale); MMSE, Mini-Mental State Examination; N, number; GRS, Genetic risk score; p-tau, phosphorylated tau; SD, standard deviation.⁹

only in the analysis comparing AT groups, and excluded from subsequent analyses that focused on AD-related processes, resulting in a final sample of 1612 individuals. Imaging-derived phenotype distributions and data availability are reported in Table S2 and Figures S1 and S2.

3.2 | Pathways in Alzheimer's disease genetic risk

Global GRSs for AD was built using 85 SNPs that were identified previously.¹ We assigned two global GRSs to each participant, one including the weighted effect of all the 85 SNPs (GRS_{APOE}), and a second one excluding the effect of the two APOE SNPs (rs7412 and rs429358; GRS_{noAPOE}). The variant-pathway mapping yielded six significant clusters (Figure 1), referred to as (1) immune activation (no. of SNPs = 27), (2) signal transduction (no. of SNPs = 48), (3) inflammation (no. of SNPs = 52), (4) migration (cholesterol and lipid related, no. of SNPs = 47), (5) amyloid (no. of SNPs = 50), and (6) clearance (no. of SNPs = 70; Figure 1). Individual pathway-GRSs were derived for each of the identified clusters. The correlation between scores in different pathway-GRSs is illustrated in Figure S3. Mapped Gene Ontology terms and relative assigned clusters are reported in Table S3. The percentages of contribution of each SNP to each pathway are reported in Table S4.

3.3 | Genetic risk and pathways determine AD CSF biomarkers

First, we assessed the influence of the GRSs on the CSF measures and the AT group classification using linear models. All models' coefficients are illustrated in Figure 2 and reported in Table S5. Association of pathway-GRSs with age and sex is illustrated in Figure S4 and S5.

Higher GRS_{APOE} was significantly related to decreased CSF A β _{1–42} (β = –0.48; FDR adjusted p < 0.001) and increased CSF p-tau₁₈₁ (β = 0.36; FDR adjusted p < 0.001). GRS_{noAPOE} showed a reduced, but still significant, association with decreased A β _{1–42} levels (β = –0.07; FDR adjusted p < 0.001), and with higher levels of p-tau₁₈₁ (β = 0.11; FDR adjusted p < 0.001). All pathway-GRSs were associated with CSF A β _{1–42} (all FDR adjusted p < 0.05), except for the migration pathway that showed a trend-level association only (FDR adjusted p = 0.08). All pathway-GRSs were also significantly associated with CSF p-tau₁₈₁, even when correcting for CSF A β _{1–42} (all FDR adjusted p < 0.05), except for the inflammation pathway that showed a trend-level association (FDR adjusted p = 0.08). When stratifying this analysis per AT group (Figure S6), we observed a stage-independent association of GRS_{APOE} with CSF A β _{1–42}, while most pathways were more strongly associated with CSF p-tau₁₈₁ in A+T– participants.

We then compared the global and pathway-GRSs between the AT groups using multinomial logistic regressions. Compared to the reference group (A–T–), all AT groups showed higher GRS_{APOE} values (all p < 0.001). Moreover, higher GRS_{noAPOE} values were observed in the A–T+ (odds ratio [OR] = 1.28; confidence interval [CI] = 1.04–1.58; p = 0.016) and in the A+T+ group (OR = 1.45; CI = 1.20–1.77; p < 0.001). Regarding the pathway-GRSs, the A–T+ group had significantly higher scores in the immune activation (OR = 1.29; CI = 1.05–1.58; p = 0.015), signal transduction (OR = 1.42; CI = 1.17–1.74; p = 0.001), and inflammatory (OR = 1.32; CI = 1.09–1.61; p = 0.014) pathway-GRSs compared to A–T–. Furthermore, the A+T– group had significantly higher clearance pathway scores (OR = 1.12; CI = 0.99–1.26; p = 0.041), whereas the A+T+ group showed significantly higher pathway-GRSs for the migration (OR = 1.26; CI = 1.04–1.53; p = 0.007), amyloid (OR = 1.45; CI = 1.19–1.76; p < 0.001), clearance (OR = 1.35; CI = 1.11–1.63; p < 0.001), and signal transduction scores (OR = 1.38; CI = 1.13–1.67; p = 0.004) compared to A–T–.

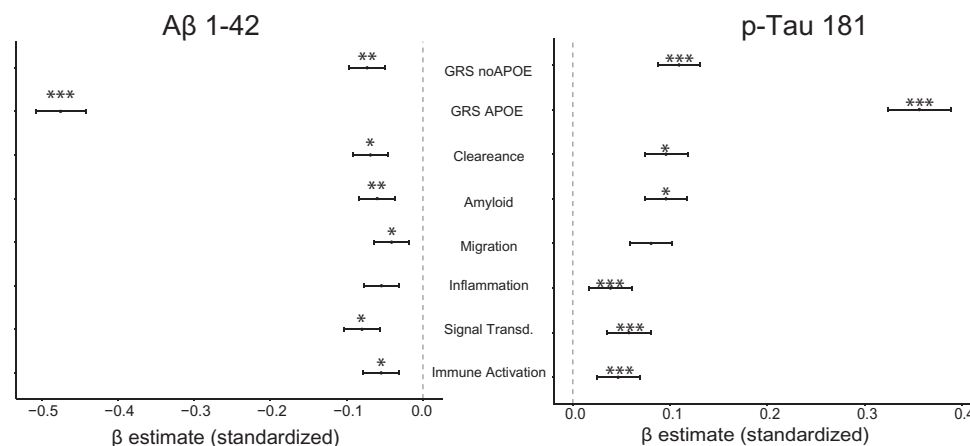


FIGURE 2 Association of global and pathway-specific genetic risk scores (pathway-GRSs) with cerebrospinal fluid (CSF) biomarkers. Forest plot reporting illustrating the association (standardized β coefficients, confidence intervals and p -values) of GRS (with and without apolipoprotein E [APOE]) and the six pathway-GRSs with CSF amyloid beta 1-42 ($A\beta_{1-42}$) phosphorylated tau (p-tau₁₈₁). * = $p < 0.05$; ** = $p < 0.005$; *** = $p < 0.001$.

3.4 | Pathways of inflammation determine cSVD radiological indices

We then investigated whether global and pathway-GRSs were related to radiological indices of cSVD, independently of AT stage. The cSVD indices included Fazekas deep (DWMH) and periventricular (PVH) enlarged perivascular spaces in basal ganglia (PVS-BG) and centrum semiovale (PVS-CS), and CMBs (supplementary materials). All model coefficients are reported in Tables S6 and S7, and illustrated in Figure 3. Briefly, participants with a Fazekas DWMH score of 2 had higher scores in GRS_{noAPOE} (OR = 1.24; CI = 1.03–1.47; $p = 0.02$) and in pathway-GRSs of signal transduction (OR = 1.26; CI = 1.05–1.50; $p = 0.01$), inflammation (OR = 1.29; CI = 1.08–1.53; $p < 0.01$), and amyloid (OR = 1.24; CI = 1.04–1.49; $p < 0.01$), compared to Fazekas DWMH = 0. A score of 1 and 2 of PVS-BG (compared to 0) was related to higher pathway-GRSs of immune activation (PVS-BG1: OR = 1.36; CI = 1.04–1.79; $p = 0.02$; PVS-BG2: OR = 1.40; CI = 1.02–1.92; $p = 0.04$); and a score of 3 of PVS-CS (compared to 0) was related to higher GRS_{APOE} (OR = 1.58; CI = 1.09–2.31; $p = 0.02$). Finally, CMBs (>2) were significantly higher in GRS_{noAPOE} (OR = 1.54; CI = 1.02–2.32; $p = 0.04$) and in pathway-GRSs of immune activation (OR = 1.32; CI = 1.03–1.70; $p = 0.02$) and signal transduction (OR = 1.31; CI = 1.02–1.68; $p = 0.04$). GRS_{APOE} (OR = 1.94; CI = 1.38–2.72; $p = 0.07$) and pathway-GRSs inflammation (OR = 1.28; CI = 1.01–2.62; $p = 0.07$) showed a statistical trend in these groups.

3.5 | Distinct genetic pathways regulate quantitative imaging biomarkers

Next, we assessed whether global and pathway-GRSs determine alterations in quantitative MRI-derived phenotypes, independently of AT stage. Model coefficients of T1w and FLAIR MRI-derived phenotypes are illustrated in Figure 4 and Table S7. Lower hippocampal volumes

showed a mild association with higher pathway-GRSs of migration and clearance, which did not survive multiple testing corrections. For WMH volumes, higher clearance pathway-GRSs were associated with higher WMH volumes in most regions. The effect was most pronounced in global, frontal, and temporal periventricular and parietal deep white matter. The association of higher GRS_{noAPOE} with higher burden of WMHs in temporal (periventricular and deep) and parietal (deep) WMHs did not survive FDR correction.

Model coefficients of rs-fMRI and DWI-derived phenotypes are illustrated in Figures 5 and 6, respectively. Lower FC within the ventral DMN was associated with higher scores in the pathway-GRSs of signal transduction. The association of ventral DMN FC with the inflammatory pathway-GRSs did not survive multiple testing corrections.

Higher GRS_{noAPOE} was associated with higher FA in the genu and lower MD in the splenium of the corpus callosum. Moreover, FA and MD were distinctively related to the migration pathway-GRSs. Specifically, increases in FA in all commissural regions of interest (ROIs; genu, body, and splenium of corpus callosum) and in the corona radiata, and decreases of MD in the cingulum, genu, and splenium of corpus callosum associated significantly with higher migration pathway-GRSs. Lower MD in the splenium of the corpus callosum also exhibited a significant association with higher scores in the immune activation and inflammation pathway-GRSs.

4 | DISCUSSION

We identified and quantified global and pathway-GRSs from genetic data in a large cohort of non-demented individuals and assessed their association with AD biomarkers. Our findings confirm the involvement of several biological pathways beyond APOE within the genetic risk of AD and demonstrate their influence on fluid and imaging biomarkers. APOE-dependent genetic risk of AD is mostly related to core AD CSF biomarkers. Beyond APOE, pathways of inflammation

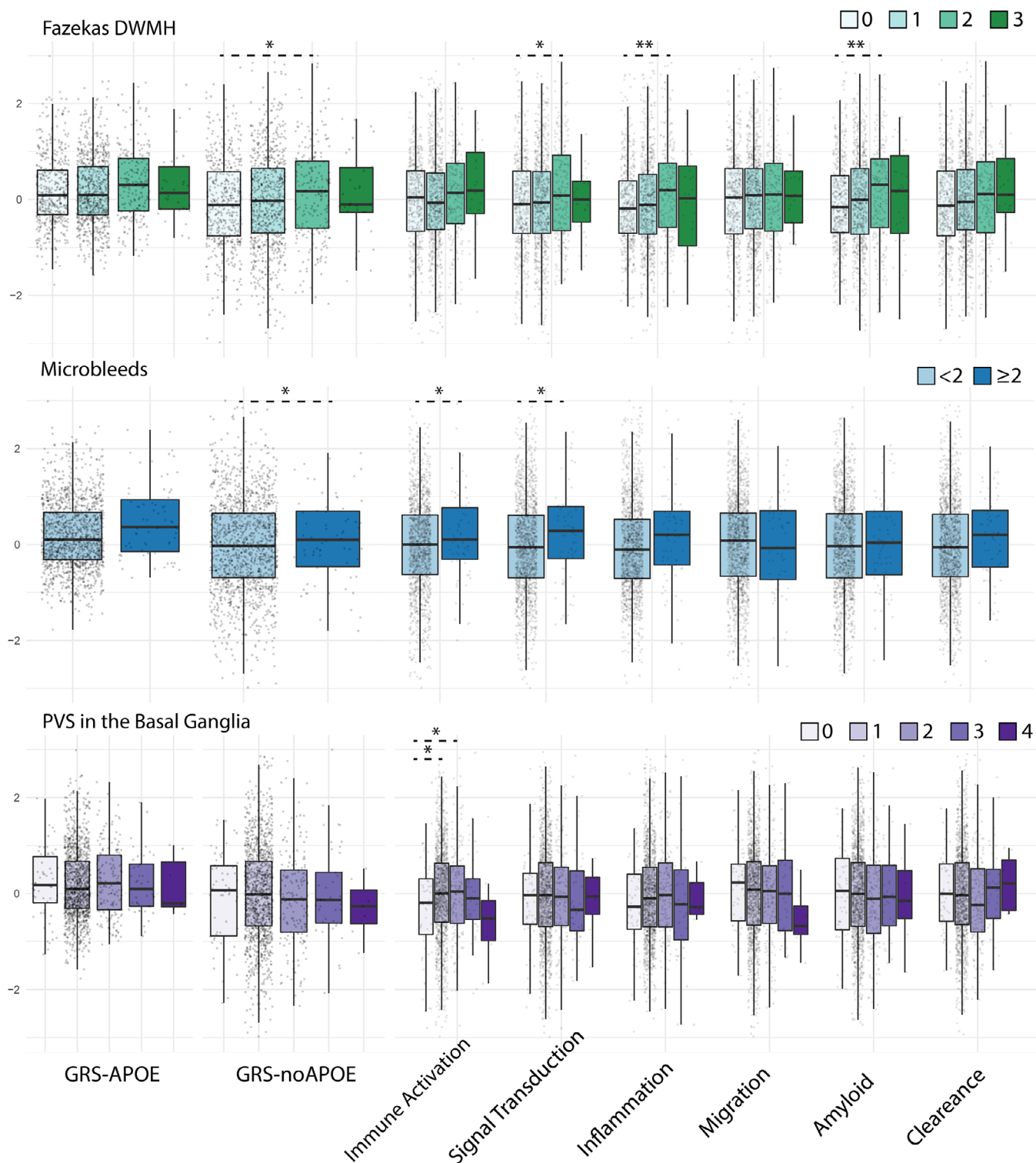


FIGURE 3 Association of global and pathway-specific genetic risk scores (pathway-GRSs) with radiological visual scores of cerebral small vessel disease (cSD). Boxplots represent the association of GRS (with and without apolipoprotein E) and the six pathway-GRSs with Fazekas deep white matter hyperintensities (DWMHs; upper-row), microbleeds (middle-row), perivascular spaces (PVSs) in the basal ganglia (lower-row). APOE, apolipoprotein E.

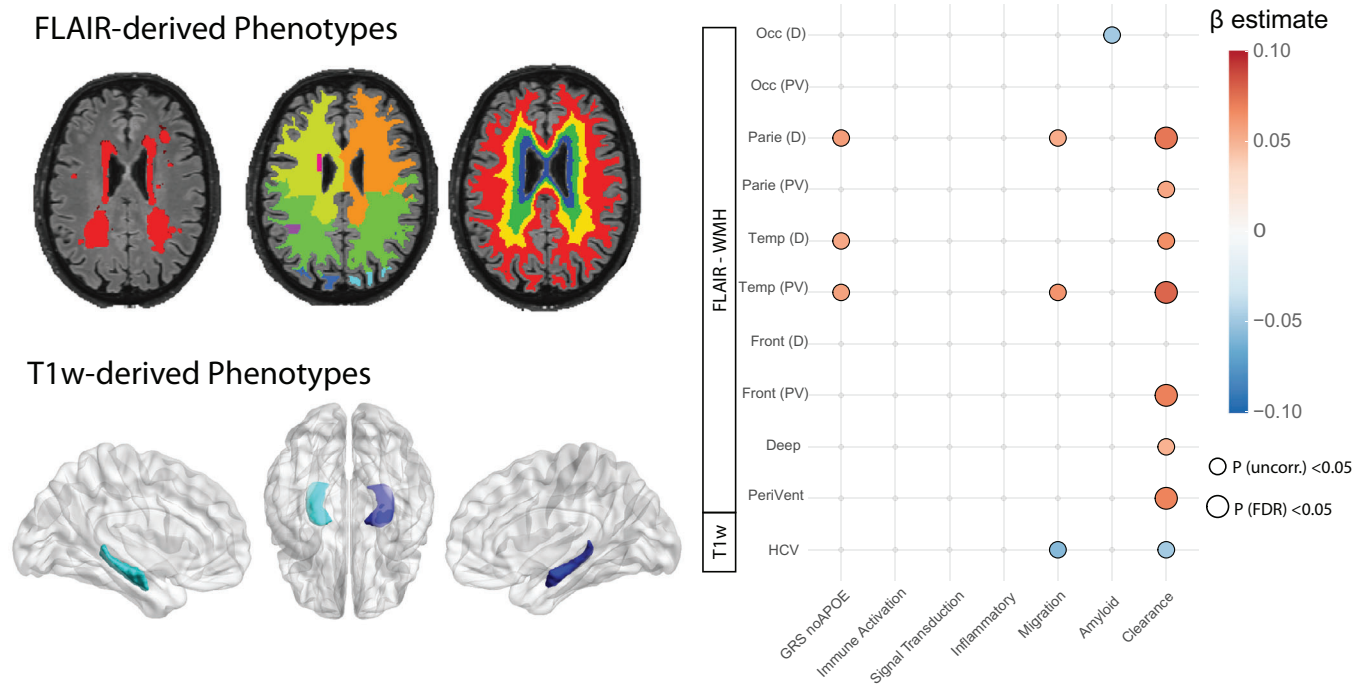


FIGURE 4 Association ($n = 1334$) of global and pathway-GRSs with FLAIR and T1w MRI-derived phenotypes. Upper-left: shows FLAIR-derived phenotypes as computed using BaMoS.²⁹ From left to right, first WMH segmentation was performed, followed by grouping WMH volumes into the four major lobes, and finally in periventricular (blue and green) and deep (yellow and red) regions, effectively providing eight regions of interest. Lower-left: T1w-derived phenotypes are obtained from the LEAP pipeline.²⁸ Right: β coefficients (colors) and p -values (circles) of linear models with global (GRS_{noAPOE}) and pathway-GRSs predicting MRI-derived phenotypes. APOE, apolipoprotein E; FLAIR, fluid-attenuated inversion recovery; T1w, T1-weighted; HCV, hippocampal volume; PeriVent, global periventricular; PV, periventricular; D, deep; Front, frontal; Temp, temporal; Parie, parietal; Occ, occipital; uncorr, uncorrected; FDR, false discovery rate; GRS, genetic risk score; MRI, magnetic resonance imaging; BaMoS, Bayesian model selection; LEAP, learning embeddings for atlas propagation.

and immune activation are specifically related to vascular imaging markers, whereas WM integrity and functional connectivity measures are mostly determined by membrane-related and signal transduction pathways, respectively.

The pathway analysis used in this work for the quantification of pathway-GRSs identified six biological pathways that are known to occur in the pathogenesis of AD from other previous studies.^{1,37-39} These pathways could be grouped into two high-level clusters (Figure 1). The first cluster, comprising immune activation, signal transduction, and inflammation pathways, mostly represents processes linked to neuroinflammatory and chronic immune activation states.⁴⁰ This confirms previous studies that reported the contribution of inflammation-related genetic variants to the development of AD,⁴¹ with a particular interest in the genes regulating microglial function, such as *TREM2* and *PLCG2*,⁴² suggesting that these pathways may constitute major non- $A\beta$ -dependent polygenetic vulnerability to AD. The second cluster, comprising the migration (related to membrane integrity and lipids), amyloid, and clearance pathways, could be representative of more AD-specific processes. Genes mostly expressed in these pathways, such as *APP*, *BIN1*, and *SORL1*, regulate processes linked to $A\beta$ production, metabolism, and endocytosis. The results of our pathway enrichment analysis provide genetic evidence of the two major pathological components in AD, namely, inflammatory and amyloid-related processes. These results are particularly interesting in

light of recent clinical trials effort, which mostly comprise $A\beta$ -targeting drugs but also see an increase of anti-inflammatory agents.⁴³

We found that global GRSs, irrespective of APOE genstatus, and most pathway-GRSs were related to CSF $A\beta_{1-42}$ burden. Whereas the early influence of the APOE $\epsilon 4$ allele and AD GRSs on amyloid burden is known,⁴⁴⁻⁴⁸ little evidence on the APOE-independent genetic influence exists.⁴⁹ Pathways of clearance and cholesterol have previously been shown to relate to CSF $A\beta_{1-42}$ in individuals genetically enriched for AD.¹¹ Endocytosis and immune response pathways have in turn often been associated with clinical and cognitive status,¹⁸ and with resilience to AD.³⁹ We showed that all GRSs and pathway-GRSs were significantly associated with CSF p-tau₁₈₁ levels, independently of CSF $A\beta_{1-42}$. Furthermore, pathway-GRSs of inflammation were specifically higher in the SNAP group, that is, the A-T+ participants, having only high CSF p-tau₁₈₁ levels and not CSF $A\beta_{1-42}$. Recent studies have demonstrated that AD GRSs excluding APOE are associated with higher CSF p-tau₁₈₁.^{16,50-52} A combined tau and amyloid PET study showed that the spread of tau pathology was regulated by “axon-related” genes, whereas the spread of amyloid was linked to “dendrite-related” genes.⁵³ Furthermore, “lipid metabolism-related” genes were driving the spread of both pathologies.⁵³ Human and animal studies have reported evidence of inflammation being present in both primary and secondary tauopathies.^{54,55} A state of chronic neuroinflammation and immune activation might not only be a reaction to neural death and

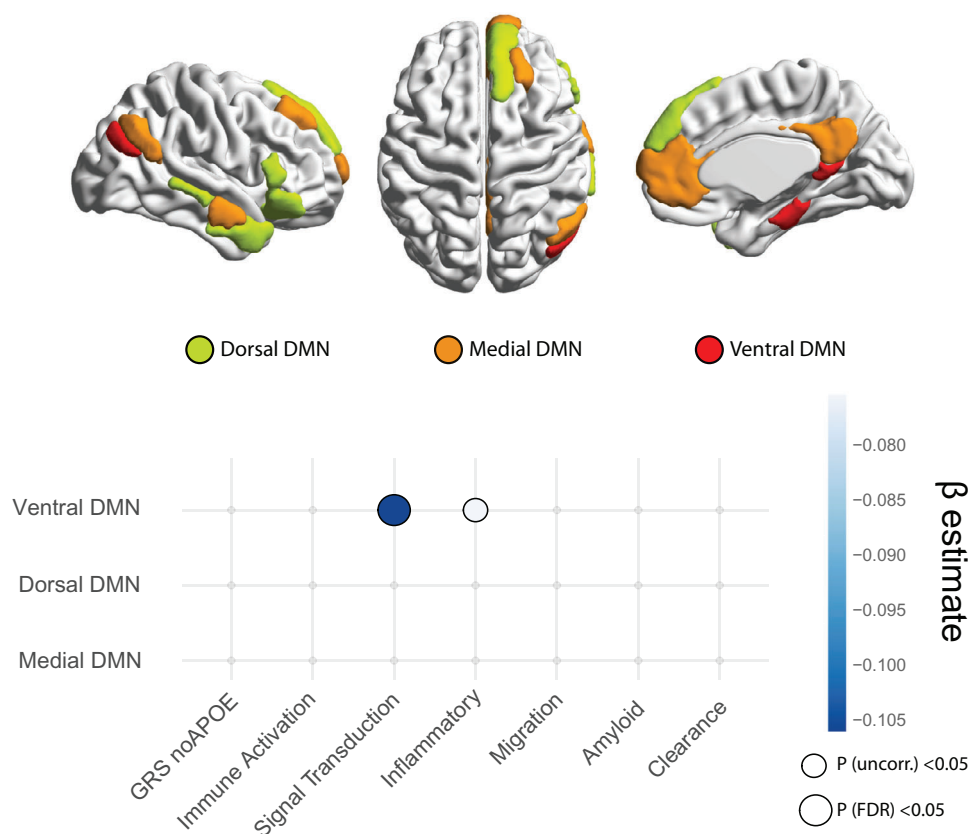


FIGURE 5 Association ($n = 776$) of global and pathway GRSs with rs-fMRI derived phenotypes. Top panel: rs-fMRI-derived phenotypes are computed as the mean within network functional connectivity in three subsystems of the DMN defined as dorsal DMN (yellow), medial DMN (orange), and ventral DMN (red). Bottom panel: the heatmap shows β coefficients (colors) and p -values (circles) of linear models with global (GRS_{noAPOE}) and pathway-GRSs predicting rs-fMRI-derived phenotypes. DMN, default mode network; GRS, genetic risk score; Uncorr, uncorrected; FDR, false discovery rate; rs-fMRI, resting-state functional magnetic resonance imaging.

misfolded proteins, but also a driver in neurodegenerative diseases. In light of these previous studies, our findings suggest that amyloid and tau deposition might be driven by alterations in several biological processes, through correlated but independent pathways, and further demonstrate that AD risk genes regulating these processes might act in parallel and upstream of both amyloid and tau. Results of our sensitivity analysis (Figure S6), further suggest that genetic pathways might have a stage-dependent influence on AD CSF biomarkers, with APOE driving initial amyloid deposition and non-APOE pathways regulating downstream processes such as tau deposition.⁵⁶ Future longitudinal studies should better investigate temporal dynamics of genetic vulnerability.

Concomitant cSVD pathology is observed in 60%–80% of patients with AD.⁵⁷ We showed the involvement of AD-related inflammatory pathways, namely, immune activation, signal transduction, and inflammation, in promoting brain vascular damage, providing evidence of a genetic overlap between cSVD and AD, and suggesting an intrinsic relationship between the two. Animal studies have demonstrated that genes coding for pro-inflammatory cytokine production led to endothelium dysfunction and damage to the brain vasculature.⁵⁸ The vulnerability of the blood–brain barrier (BBB) to the effects of chronic immune activation and inflammation⁴⁰ results in alterations of the neurovascular unit with advancing age. This observation suggests that

innate inflammatory processes might foster AD pathology by promoting vascular damage and BBB disruption, from the early stages of the disease. Of note, these associations were stronger for intermediate radiological scores. This could be due to the limited number of participants with significant cerebrovascular burden. However, specific inflammation-related pathways may play a role in the initial onset of cSVD, whereas a combination of various altered biological processes could be at play in later stages.

Using quantitative MRI markers, we found that specific imaging biomarkers might be influenced by distinct genetic pathways. Recent research has linked several pathway-GRSs with cortical thinning and in several brain regions, including the hippocampus.⁵⁹ We found that lower volumes in the hippocampus were mildly associated with higher scores in pathway-GRSs of migration and clearance. In addition, WM lesion volumes—reflecting demyelination and axonal loss,⁶⁰ commonly considered a result of heterogeneous causes, primarily cSVD⁶⁰—were specifically determined by the clearance pathway-GRSs. The glymphatic system plays a central role in maintaining WM integrity by preserving the flow of interstitial fluid and exchanging metabolic waste.⁶¹ In previous works, the *CLU* gene, associated with the clearance of cellular debris and apoptosis, and the *PICALM* gene, involved in clathrin-mediated endocytosis, were associated with WMHs.¹⁸ Poly-

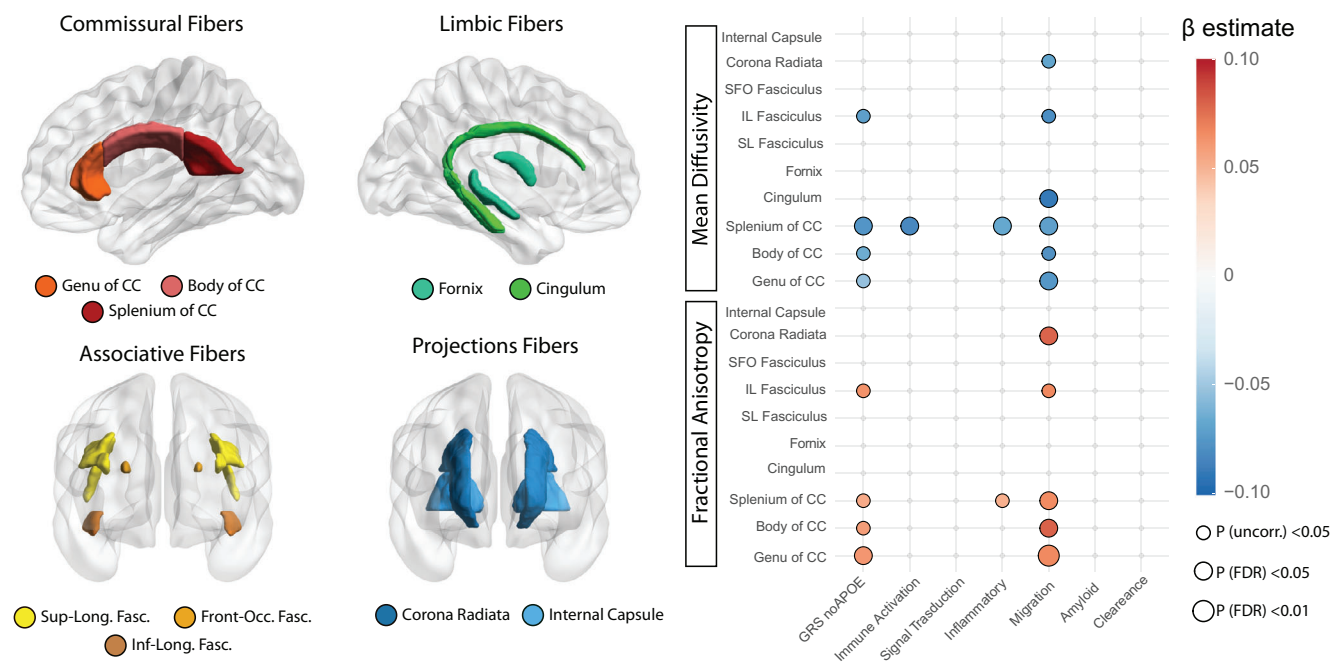


FIGURE 6 Association ($n = 790$) of global and pathway-GRSs with DWI-derived phenotypes. Left panel: DWI-derived phenotypes are computed through TBSS pipeline as mean FA and MD within 10 regions of interest including commissural (genu, body, and splenium of CC), limbic (fornix and cingulum), associative (superior longitudinal, fronto-occipital and inferior longitudinal fasciculi), and projection (corona radiata and internal capsule) white matter tracts. Right panel: the heatmap shows β coefficients (colors) and p values (circles) of linear models with global (GRS_{noAPOE}) and pathway-GRSs predicting DWI-derived phenotypes. CC, corpus callosum; Sup-Long(SL), superior longitudinal; Front-Occ(SFO), fronto-occipital; Inf-Long(IL), inferior longitudinal; Fasc, fasciculus; Uncorr, uncorrected; FDR, false discovery rate; DWI, diffusion-weighted imaging; TBSS, tract-based spatial statistics; FA, fractional anisotropy; MD, mean diffusivity; GRS, genetic risk score.

genetic variants regulating the glymphatic system might promote AD pathology through WM damage, and WMHs could be both the consequence and the cause of glymphatic dysfunction.⁶¹ DWI-derived imaging—reflecting WM microstructural integrity—were mostly determined by the migration GRSs, linked to cholesterol and lipid dysfunction. Previous work has shown that levels of local cholesterol and lipid metabolism can regulate WM integrity, as measured on DWI, by regulating WM myelination.⁶² Cholesterol dysmetabolism is thought to interact with WM demyelination to promote and worsen initial amyloid pathology.⁶³ Our results provide genetic evidence for the role of early cholesterol and lipid dysmetabolism and WM injury in the pre-dementia stages of AD.

The signal transduction pathway-GRS, involving synaptic function and intracellular communication, was related to rs-fMRI as reduced FC in the dorsal portion of the DMN. Among the genes mostly contributing to this pathway, *SORL1*, *BIN1*, and *CD2AP* are functionally expressed in pre- and post-synaptic compartments and promote synaptic formation, transmission, and plasticity. Alterations of synaptic function (and functional connectivity on fMRI) are observable early in the AD continuum,^{64,65} and have been proposed to be a driving event in the disease course.³³ In this framework, large-scale reconfiguration of functional networks in aging brains would influence biological processes linked to amyloid production.⁶⁶ We, therefore, showed that a specific cluster of variants could promote AD pathology by acting on functional brain alterations and neuronal activity.

Some limitations should be noted. First, the computation of GRSs is based on a reference GWAS that used “Alzheimer’s disease and related dementias” as a phenotype. However, this method was shown to be sensitive and effective in increasing the number of included participants in the GWAS, thereby increasing the sensitivity (more loci) and precision of the obtained estimates. Second, the method used to identify pathways-GRSs did not constrain genes’ contribution to only one cluster (one gene could contribute to multiple pathways). As such, some pathway-GRSs were more related to each other (supplementary materials). Other methods exist for computation of pathway-GRSs, often assigning genes to a priori selected sets of pathways.^{59,67} However, single genes can contribute to multiple biological processes. Moreover, the observation that GRSs had different profiles of associations with outcome biomarkers advocates for distinct underlying processes. Future studies should assess the independent contribution of pathway-GRSs to imaging phenotypes. Moreover, future works should also investigate the cell-type expression profiles of at-risk genes.^{68,69} Finally, we only considered one gene per SNP, as reported in the original GWAS. Although snpXplorer is robust in pathway identification over a series of annotation strategies,²² more studies are needed to evaluate different gene identification approaches and compare the results.

Taken together, our results demonstrate that the genetic risk for AD is associated with a broad range of neuropathological features in non-demented individuals that can be tracked in vivo through neuroimaging techniques, and that distinct AD biomarkers are preferentially

associated with specific genetic profiles. Our findings are a step forward in the understanding of the biological alterations that determine brain functional and structural dysregulation in the early stages of the AD continuum. Moreover, these results provide genetic evidence of the biological pathways promoting disease heterogeneity and offer novel insights into the use of individual risk profiles for patient selection in clinical trials and personalized interventions, encompassing a combination of strategies targeting modifiable risk factors, alongside non-amyloid-targeting drugs.

AFFILIATIONS

¹Department of Radiology and Nuclear Medicine, Amsterdam University Medical Centre, Vrije Universiteit, Amsterdam, The Netherlands

²Amsterdam Neuroscience, Brain Imaging, Amsterdam, The Netherlands

³Clinical Memory Research Unit, Department of Clinical Sciences Malmö, Lund University, Lund, Sweden

⁴Genomics of Neurodegenerative Diseases and Aging, Human Genetics, Vrije Universiteit Amsterdam, Amsterdam, The Netherlands

⁵Delft Bioinformatics Lab, Delft University of Technology, Delft, The Netherlands

⁶Barcelonaβeta Brain Research Center (BBRC), Pasqual Maragall Foundation, Barcelona, Spain

⁷Universitat Pompeu Fabra, Barcelona, Spain

⁸Centre for Genomic Regulation (CRG), The Barcelona Institute for Science and Technology, Barcelona, Spain

⁹Department of Clinical Genetics, Erasmus University Medical Center, Rotterdam, The Netherlands

¹⁰Department of Radiology, Copenhagen University Hospital Rigshospitalet, Copenhagen, Denmark

¹¹Cerebriu A/S, Copenhagen, Denmark

¹²Department of Psychiatry and Neurochemistry, Institute of Neuroscience and Physiology, the Sahlgrenska Academy at the University of Gothenburg, Mölndal, Sweden

¹³Clinical Neurochemistry Laboratory, Sahlgrenska University Hospital, Mölndal, Sweden

¹⁴GE Healthcare, Amersham, UK

¹⁵Laboratory Alzheimer's Neuroimaging & Epidemiology, IRCCS Istituto Centro San Giovanni di Dio Fatebenefratelli, Brescia, Italy

¹⁶University Hospitals and University of Geneva, Geneva, Switzerland

¹⁷CIMC - Centre d'Imagerie Médicale de Cornavin, Geneva, Switzerland

¹⁸Department of Surgical Sciences, Radiology, Uppsala University, Uppsala, Sweden

¹⁹Department of Radiology, Beijing Tiantan Hospital, Capital Medical University, Beijing, P. R. China

²⁰Alzheimer Center Amsterdam, Department of Neurology, Amsterdam Neuroscience, Vrije Universiteit Amsterdam, Amsterdam, The Netherlands

²¹Centro de Investigación y Terapias Avanzadas, Neurología, CITA-Alzheimer Foundation, San Sebastián, Spain

²²Centre for Genomic and Experimental Medicine, Institute of Genetics and Cancer, University of Edinburgh, Edinburgh, UK

²³Department of Psychiatry, School of Clinical Medicine, University of Cambridge, Cambridge, UK

²⁴Life and Health Sciences Research Institute (ICVS), School of Medicine, University of Minho, Braga, Portugal

²⁵ICVS/3B's - PT Government Associate Laboratory, Braga/Guimarães, Portugal

²⁶Department of Nuclear Medicine, Toulouse University Hospital, Toulouse, France

²⁷ToNIC, Toulouse NeuroImaging Center, University of Toulouse, Inserm, Toulouse, France

²⁸Edinburgh Dementia Prevention, Centre for Clinical Brain Sciences, Outpatient Department 2, Western General Hospital, University of Edinburgh, Edinburgh, UK

²⁹Brain Health Scotland, Edinburgh, UK

³⁰Takeda Pharmaceuticals Ltd., Cambridge, Massachusetts, USA

³¹Department of Medical Physics and Biomedical Engineering, Centre for Medical Image Computing (CMIC), University College London (UCL), London, UK

³²MRC Unit for Lifelong Health & Ageing at UCL, University College London, London, UK

³³School of Biomedical Engineering and Imaging Sciences, King's College London, London, UK

³⁴Centre for Clinical Brain Sciences, The University of Edinburgh, Edinburgh, UK

³⁵Department of Medicine, Imperial College London, London, UK

³⁶IXICO, London, UK

³⁷Université de Normandie, Unicaen, Inserm, U1237, PhIND "Physiopathology and Imaging of Neurological Disorders", institut Blood-and-Brain @ Caen-Normandie, Cycleron, Caen, France

³⁸German Center for Neurodegenerative Diseases (DZNE), Munich, Germany

³⁹Ghent Institute for Functional and Metabolic Imaging (GlfMI), Ghent University, Ghent, Belgium

⁴⁰CIBER Bioingeniería, Biomateriales y Nanomedicina (CIBER-BBN), Madrid, Spain

⁴¹IMIM (Hospital del Mar Medical Research Institute), Barcelona, Spain

⁴²Amsterdam Neuroscience, Neurodegeneration, Amsterdam, The Netherlands

⁴³Alzheimer Center Limburg, Department of Psychiatry & Neuropsychology, School of Mental Health and Neuroscience, Maastricht University, Maastricht, The Netherlands

⁴⁴Division of Neurogeriatrics, Department of Neurobiology, Care Sciences and Society, Karolinska Institutet, Stockholm, Sweden

⁴⁵Centre for Medical Image Computing, Department of Medical Physics and Biomedical Engineering, University College London, London, UK

⁴⁶Institutes of Neurology and Healthcare Engineering, University College London, London, UK

ACKNOWLEDGMENTS

This work is part of the EPAD LCS (European Prevention of Alzheimer's Dementia Longitudinal Cohort Study). The authors would like to express their most sincere gratitude to the EPAD LCS participants, without whom this research would have not been possible. This work has received support from the EU/EFPIA Innovative Medicines Initiative Joint Undertaking EPAD grant agreement nr. 115736

CONFLICT OF INTEREST STATEMENT

EPAD is supported by the EU/EFPIA Innovative Medicines Initiative (IMI) grant agreement 115736.

The project leading to this paper has received funding from the Innovative Medicines Initiative (IMI) 2 Joint Undertaking under grant agreement No 115952. This Joint Undertaking receives the support from the European Union's Horizon 2020 research and innovation programme and European Federation of Pharmaceutical Industries Association (EFPIA). This communication reflects the views of the authors, and

neither IMI nor the European Union (EU) and EFPIA are liable for any use that may be made of the information contained herein. A.M.W., H.M., L.E.C., and F.B. are supported by AMYPAD (IMI 115952). H.M. is supported by the Dutch Heart Foundation (2020T049), the Eurostars-2 joint programme with co-funding from the European Union Horizon 2020 research and innovation programme (ASPIRE E!113701), provided by the Netherlands Enterprise Agency (RvO), and by the EU Joint Program for Neurodegenerative Disease Research, provided by the Netherlands Organisation for Health Research and Development and Alzheimer Nederland (DEBBIE JPND2020-568-106). F.B. is supported by Engineering and Physical Sciences Research Council (EPSRC), EU-JU (IMI), National Institute for Health and Care Research - Biomedical Research Center (NIHR-BRC), General Electric (GE) HealthCare, and Alzheimer's Disease Data Initiative (ADDI; paid to institution); is a consultant for Combinostics, IXICO, and Roche; participates on advisory boards of Biogen, Prothena, and Merck; and is a co-founder of Queen Square Analytics. L.E.C. has received research support from GE HealthCare Ltd. (paid to institution). C.F. is an employee of GE HealthCare Ltd. P.H.S. is a full-time employee of EQT Life Sciences (formerly LSP) and professor emeritus at Amsterdam University Medical Centers. He has received consultancy fees (paid to the university) from Alzhon, Brainstorm Cell, and Green Valley. Within his university affiliation, he is global principal investigator of the Phase 1b study of AC Immune, Phase 2b study with FUJI-film/Toyama, and Phase 2 study of UCB. He is past chair of the EU steering committee of the Phase 2b program of Vivoryon and the Phase 2b study of Novartis Cardiology, and he is presently co-chair of the Phase 3 study with NOVO-Nordisk. R.W. is an employee of IXICO. C.R. has done paid consultancy work in the last 3 years for Eli Lilly, Biogen, Actinogen, Brain Health Scotland, Roche, Roche Diagnostics, Novo Nordisk, Eisai, Signant, Merck, Alchemab, Sygnaure, and Abbvie. His group has received Research Income for his Research Unit from Biogen, AC Immune, and Roche. He has out-licensed IP developed at the University of Edinburgh to Linus Health and is chief executive officer (CEO) and Founder of Scottish Brain Sciences. S.H. is a consultant for WYSS Center, Geneva, Switzerland, and a consultant for SPINEART, Geneva, Switzerland. G.C. has received research support from the European Union's Horizon 2020 research and innovation programme (grant agreement number 667696), Fondation d'entreprise MMA des Entrepreneurs du Futur, Fondation Alzheimer, Agence Nationale de la Recherche, Région Normandie, Association France Alzheimer et maladies apparentées, Fondation Vaincre Alzheimer, Fondation Recherche Alzheimer, and Fondation pour la Recherche Médicale (all to Inserm), and personal fees from Inserm and Fondation Alzheimer. A.J.S. is an employee and minor shareholder of Takeda Pharmaceutical Company Ltd. J.O.B. has acted as a consultant for TauRx, Novo Nordisk, Biogen, Roche, Lilly, and GE Healthcare; and received grant support from Avid/ Lilly, Merck, and Alliance Medical.

R.E.M. has received a speaker fee from Illumina; is an advisor to the Epigenetic Clock Development Foundation; and has received consultant fees from Optima partners. Author disclosures are available in the [supporting information](#).

CONSENT STATEMENT

All EPAD participants provided written informed consent.

ORCID

Luigi Lorenzini  <https://orcid.org/0000-0002-9756-881X>

REFERENCES

- Bellenguez C, Küçükali F, Jansen IE, et al. New insights into the genetic etiology of Alzheimer's disease and related dementias. *Nat Genet.* 2022;54:412-436.
- Sims R, Hill M, Williams J. The multiplex model of the genetics of Alzheimer's disease. *Nat Neurosci.* 2020;23:311-322.
- Ferreira D, Nordberg A, Westman E. Biological subtypes of Alzheimer disease: a systematic review and meta-analysis. *Neurology.* 2020;94:436-448.
- Dong A, Toledo JB, Honnorat N, et al. Heterogeneity of neuroanatomical patterns in prodromal Alzheimer's disease: links to cognition, progression and biomarkers. *Brain.* 2017;140:735-747.
- Scheltens P, Blennow K, Breteler MMB, et al. Alzheimer's disease. *Lancet.* 2016;388:505-517.
- Ten Kate M, Dicks E, Visser PJ, et al. Atrophy subtypes in prodromal Alzheimer's disease are associated with cognitive decline. *Brain.* 2018;141:3443-3456.
- Mehta D, Jackson R, Paul G, Shi J, Sabbagh M. Why do trials for Alzheimer's disease drugs keep failing? A discontinued drug perspective for 2010-2015. *Expert Opin Investig Drugs.* 2017;26:735-739.
- Wesnesen KEJ, Teunissen CE, Visser PJ, Tijms BM. Cerebrospinal fluid proteomics and biological heterogeneity in Alzheimer's disease: a literature review. *Crit Rev Clin Lab Sci.* 2020;57:86-98.
- Lam B, Masellis M, Freedman M, Stuss DT, Black SE. Clinical, imaging, and pathological heterogeneity of the Alzheimer's disease syndrome. *Alzheimer's Res Ther.* 2013;5:1. doi:10.1186/alzrt155
- Choi SW, Mak TS-H, O'Reilly PF. Tutorial: a guide to performing polygenic risk score analyses. *Nat Protoc.* 2020;15:2759-2772.
- Darst BF, Kosciak RL, Racine AM, et al. Pathway-specific polygenic risk scores as predictors of amyloid- β deposition and cognitive function in a sample at increased risk for Alzheimer's disease. *J Alzheimers Dis.* 2017;55:473-484.
- Morris JC, Roe CM, Xiong C, et al. APOE predicts amyloid-beta but not tau Alzheimer pathology in cognitively normal aging. *Annals of Neurology.* 2010;67:122-131. doi:10.1002/ana.21843
- Benson GS, Bauer C, Hausner L, et al. Don't forget about tau: the effects of ApoE4 genotype on Alzheimer's disease cerebrospinal fluid biomarkers in subjects with mild cognitive impairment—data from the dementia competence network. *J Neural Transm.* 2022;129:477-486. doi:10.1007/s00702-022-02461-0
- Mishra S, Blazey TM, Holtzman DM, et al. Longitudinal brain imaging in preclinical Alzheimer disease: impact of APOE ϵ 4 genotype. *Brain.* 2018;141:1828-1839.
- Cacciaglia R, Operto G, Falcón C, et al. Genotypic effects of APOE- ϵ 4 on resting-state connectivity in cognitively intact individuals support functional brain compensation. *Cereb Cortex.* 2022;33:2748-2760. doi:10.1093/cercor/bhac239
- Altmann A, Scelsi MA, Shoai M, et al. A comprehensive analysis of methods for assessing polygenic burden on Alzheimer's disease pathology and risk beyond APOE. *Brain Commun.* 2020;2:fcz047.
- Rubinski A, Frerich S, Malik R, et al. Polygenic effect on tau pathology progression in Alzheimer's disease. *Ann Neurol.* 2023;93:819-829.
- Ahmad S, Bannister C, van der Lee SJ, et al. Disentangling the biological pathways involved in early features of Alzheimer's disease in the Rotterdam Study. *Alzheimers Dement.* 2018;14:848-857.
- Ritchie CW, Muniz-Terrera G, Kivipelto M, Solomon A, Tom B, Molinuevo JL. The European Prevention of Alzheimer's Dementia

- (EPAD) longitudinal cohort study: baseline data release V500.0. *J Prev Alzheimers Dis*. 2020;7:8-13.
20. Solomon A, Kivipelto M, Molinuevo JL, Tom B, Ritchie CW, EPAD Consortium. European Prevention of Alzheimer's Dementia Longitudinal Cohort Study (EPAD LCS): study protocol. *BMJ Open*. 2019;8:e021017.
 21. Das S, Forer L, Schönherr S, et al. Next-generation genotype imputation service and methods. *Nat Genet*. 2016;48:1284-1287.
 22. Tesi N, van der Lee S, Hulsman M, Holstege H, Reinders MJT. snpXplorer: a web application to explore human SNP-associations and annotate SNP-sets. *Nucleic Acids Res*. 2021;49:W603-W612.
 23. Raudvere U, Kolberg L, Kuzmin I, et al. g:Profiler: a web server for functional enrichment analysis and conversions of gene lists (2019 update). *Nucleic Acids Res*. 2019;47:W191-W198. doi:10.1093/nar/gkz369
 24. Ashburner M, Ball CA, Blake JA, et al. Gene ontology: tool for the unification of biology. *Nat Genet*. 2000;25:25-29.
 25. Lin D. An information-theoretic definition of similarity. *ICML*. 1998;98:296-304.
 26. Ingala S, De Boer C, Masselink LA, et al. Application of the ATN classification scheme in a population without dementia: findings from the EPAD cohort. *Alzheimers Dement*. 2021;17:1189-1204. doi:10.1002/alz.12292
 27. Lorenzini L, Ingala S, Wink AM, et al. The Open-Access European Prevention of Alzheimer's Dementia (EPAD) MRI dataset and processing workflow. *Neuroimage Clin*. 2022;35:103106.
 28. Wolz R, Aljabar P, Hajnal JV, Hammers A, Rueckert D. Alzheimer's Disease Neuroimaging Initiative. LEAP: learning embeddings for atlas propagation. *Neuroimage*. 2010;49:1316-1325.
 29. Sudre CH, Cardoso MJ, Bouvy WH, Biessels GJ, Barnes J, Ourselin S. Bayesian model selection for pathological neuroimaging data applied to white matter lesion segmentation. *IEEE Trans Med Imaging*. 2015;34:2079-2102.
 30. Pålhaugen L, Sudre CH, Tecelao S, et al. Brain amyloid and vascular risk are related to distinct white matter hyperintensity patterns. *J Cereb Blood Flow Metab*. 2020; 41:1162-1174. doi:10.1177/0271678X20957604
 31. Nickerson LD, Smith SM, Öngür D, Beckmann CF. Using dual regression to investigate network shape and amplitude in functional connectivity analyses. *Front Neurosci*. 2017;11:115. doi:10.3389/fnins.2017.00115
 32. Yeo BTT, Thomas Yeo BT, Krienen FM, et al. The organization of the human cerebral cortex estimated by intrinsic functional connectivity. *J Neurophysiol*. 2011;106:1125-1165. doi:10.1152/jn.00338.2011
 33. Jones DT, Knopman DS, Gunter JL, et al. Cascading network failure across the Alzheimer's disease spectrum. *Brain*. 2016;139:547-562.
 34. Wardlaw JM, Smith EE, Biessels GJ, et al. Neuroimaging standards for research into small vessel disease and its contribution to ageing and neurodegeneration. *Lancet Neurol*. 2013;12:822-838. doi:10.1016/s1474-4422(13)70124-8
 35. MacLulich AMJ, Wardlaw JM, Ferguson KJ, Starr JM, Seckl JR, Deary IJ. Enlarged perivascular spaces are associated with cognitive function in healthy elderly men. *J Neurol Neurosurg Psychiatry*. 2004;75:1519-1523.
 36. Fazekas F, Chawluk JB, Alavi A, Hurtig HI, Zimmerman RA. MR signal abnormalities at 1.5 T in Alzheimer's dementia and normal aging. *AJR Am J Roentgenol*. 1987;149:351-356.
 37. Hardy J, Bogdanovic N, Winblad B, et al. Pathways to Alzheimer's disease. *J Intern Med*. 2014;275:296-303.
 38. Van Cauwenberghe C, Van Broeckhoven C, Sleegers K. The genetic landscape of Alzheimer disease: clinical implications and perspectives. *Genet Med*. 2016;18:421-430.
 39. Tesi N, Van Der Lee SJ, Hulsman M, et al. Immune response and endocytosis pathways are associated with the resilience against Alzheimer's disease. *Alzheimers Dement*. 2020;16:332. doi:10.1002/alz.042614
 40. Newcombe EA, Camats-Perna J, Silva ML, Valmas N, Huat TJ, Medeiros R. Inflammation: the link between comorbidities, genetics, and Alzheimer's disease. *J Neuroinflammation*. 2018;15:276.
 41. Naj AC, Schellenberg GD, Alzheimer's Disease Genetics Consortium (ADGC). Genomic variants, genes, and pathways of Alzheimer's disease: an overview. *Am J Med Genet B Neuropsychiatr Genet*. 2017;174:5-26.
 42. Efthymiou AG, Goate AM. Late onset Alzheimer's disease genetics implicates microglial pathways in disease risk. *Mol Neurodegener*. 2017;12:43.
 43. Cummings J, Zhou Y, Lee G, Zhong K, Fonseca J, Cheng F. Alzheimer's disease drug development pipeline: 2023. *Alzheimers Dement*. 2023;9:e12385.
 44. Toledo JB, Habes M, Sotiras A, et al. APOE effect on amyloid- β PET spatial distribution, deposition rate, and cut-points. *J Alzheimers Dis*. 2019;69:783-793.
 45. Lim YY, Mormino EC. Alzheimer's disease neuroimaging initiative. APOE genotype and early β -amyloid accumulation in older adults without dementia. *Neurology*. 2017;89:1028-1034.
 46. Luckett ES, Abakkouy Y, Reinartz M, et al. Association of Alzheimer's disease polygenic risk scores with amyloid accumulation in cognitively intact older adults. *Alzheimers Res Ther*. 2022;14:138.
 47. Leonenko G, Shoi M, Bellou E, et al. Genetic risk for Alzheimer disease is distinct from genetic risk for amyloid deposition. *Ann Neurol*. 2019;86:427-435.
 48. Belloy ME, Napolioni V, Greicius MD. A quarter century of APOE and Alzheimer's disease: progress to date and the path forward. *Neuron*. 2019;101:820-838.
 49. Xicota L, Gyorgy B, Grenier-Boley B, et al. Association of APOE-independent Alzheimer disease polygenic risk score with brain amyloid deposition in asymptomatic older adults. *Neurology*. 2022;99:e462-e475.
 50. Louwersheimer E, Wolfgruber S, Espinosa A, et al. Alzheimer's disease risk variants modulate endophenotypes in mild cognitive impairment. *Alzheimers Dement*. 2016;12:872-881.
 51. Zettergren A, Lord J, Ashton NJ, et al. Association between polygenic risk score of Alzheimer's disease and plasma phosphorylated tau in individuals from the Alzheimer's disease neuroimaging initiative. *Alzheimers Res Ther*. 2021;13:17.
 52. Kumar A, Janelidze S, Stomrud E, et al. β -Amyloid-dependent and -independent genetic pathways regulating CSF tau biomarkers in Alzheimer disease. *Neurology*. 2022;99:e476-e487. doi:10.1212/wnl.0000000000200605
 53. Sepulcre J, Grothe MJ, d'Oleire Uquillas F, et al. Neurogenetic contributions to amyloid beta and tau spreading in the human cortex. *Nat Med*. 2018;24:1910-1918.
 54. Ising C, Heneka MT. Chronic inflammation: a potential target in tauopathies. *Lancet Neurol*. 2023;22:371-373.
 55. Langworth-Green C, Patel S, Jaunmuktane Z, et al. Chronic effects of inflammation on tauopathies. *Lancet Neurol*. 2023;22:430-442.
 56. Altmann A, Aksman LM, Oxtoby NP, ... & Oxtoby NP. Towards cascading genetic risk in Alzheimer's disease. *Brain*. 2024, awae176.
 57. Kim SE, Kim HJ, Jang H, et al. Interaction between Alzheimer's disease and cerebral small vessel disease: a review focused on neuroimaging markers. *Int J Mol Sci*. 2022;23:10490. doi:10.3390/ijms231810490
 58. Theofilis P, Sagris M, Oikonomou E, et al. Inflammatory mechanisms contributing to endothelial dysfunction. *Biomedicines*. 2021;9:781. doi:10.3390/biomedicines9070781
 59. Harrison JR, Foley SF, Baker E, et al. Pathway-specific polygenic scores for Alzheimer's disease are associated with changes in brain structure in younger and older adults. *Brain Commun*. 2023;5:fcad229.
 60. Prins ND, Scheltens P. White matter hyperintensities, cognitive impairment and dementia: an update. *Nat Rev Neurol*. 2015;11:157-165.

61. Sabayan B, Westendorp RGJ. Neurovascular-glymphatic dysfunction and white matter lesions. *GeroScience*. 2021;43:1635-1642.
62. Williams VJ, Leritz EC, Shepel J, et al. Interindividual variation in serum cholesterol is associated with regional white matter tissue integrity in older adults. *Hum Brain Mapp*. 2013;34:1826-1841.
63. Sharp FR, DeCarli CS, Jin L-W, Zhan X. White matter injury, cholesterol dysmetabolism, and APP/Abeta dysmetabolism interact to produce Alzheimer's disease (AD) neuropathology: a hypothesis and review. *Front Aging Neurosci*. 2023;15:1096206.
64. Lorenzini L, Ingala S, Collij LE, Wottschel V, Haller S, Blennow K, ... & Wink AM. Eigenvector centrality dynamics are related to Alzheimer's disease pathological changes in non-demented individuals. *Brain communications*. 2023;5(3):fcad088.
65. Damoiseaux JS, Beckmann CF, Arigita EJS, et al. Reduced resting-state brain activity in the "default network" in normal aging. *Cereb Cortex*. 2007;18:1856-1864.
66. Bero AW, Yan P, Roh JH, et al. Neuronal activity regulates the regional vulnerability to amyloid- β deposition. *Nat Neurosci*. 2011;14:750-756.
67. Choi SW, García-González J, Ruan Y, et al. PRSet: pathway-based polygenic risk score analyses and software. *PLoS Genet*. 2023;19:e1010624.
68. Blumenfeld J, Yip O, Kim MJ, Huang Y. Cell type-specific roles of APOE4 in Alzheimer disease. *Nat Rev Neurosci*. 2024;25:91-110.
69. Yang H-S, Teng L, Kang D, et al. Cell-type-specific Alzheimer's disease polygenic risk scores are associated with distinct disease processes in Alzheimer's disease. *Nat Commun*. 2023;14:7659.

SUPPORTING INFORMATION

Additional supporting information can be found online in the Supporting Information section at the end of this article.

How to cite this article: Lorenzini L, Collij LE, Tesi N, et al. Alzheimer's disease genetic pathways impact cerebrospinal fluid biomarkers and imaging endophenotypes in non-demented individuals. *Alzheimer's Dement*. 2024;20:6146-6160. <https://doi.org/10.1002/alz.14096>